Geminal-atom catalysis for efficient cross-coupling reactions

Xiao Hai[1,10], Yang Zheng[1,10], Qi Yu[2,10], Na Guo[3,10], Shibo Xi[4], Xiaoxu Zhao[5], Sharon Mitchell[6], Mu Wang[1], Xiangdong Long[1], Jing Li[1], Peng He[1], Huihui Lin[1], Yige Cui[1], Jiwei Shi[1], Jie Wu[1], Chun Zhang[3], Javier Pérez-Ramírez[6*], Ye Zhu[1*], Jun Li[7,8*] and Jiong Lu[1,9*]*

[1]Department of Chemistry, National University of Singapore, 3 Science Drive 3, Singapore 117543, Singapore.

[2]School of Materials Science and Engineering, Shaanxi University of Technology, Hanzhong 723001, China.

[3]Department of Physics, National University of Singapore, 2 Science Drive 3, Singapore, 117542, Singapore.

[4]Institute of Chemical and Engineering Sciences, Agency for Science, Technology and Research, Singapore 627833, Singapore.

[5]School of Materials Science and Engineering, Peking University, Beijing 100871, China.

[6]Institute for Chemical and Bioengineering, Department of Chemistry and Applied Biosciences, ETH Zurich, Zurich, Switzerland.

[7]Department of Chemistry, Southern University of Science and Technology, Shenzhen 518055, China.

[8]Department of Chemistry and Key Laboratory of Organic Optoelectronics & Molecular Engineering of the Ministry of Education, Tsinghua University, Beijing 100084, China.

[9]Institute for Functional Intelligent Materials, National University of Singapore, 117544, Singapore.

[10]These authors contributed equally: Xiao Hai, Yang Zheng, Qi Yu, Na Guo.

[*]E-mails: xi_shibo@partner.nus.edu.sg; junli@tsinghua.edu.cn; jpr@chem.ethz.ch; chmzhu@nus.edu.sg; chmluj@nus.edu.sg

Abstract

The presence of well-defined active sites in single-atom catalysts (SAC) triggers interest in their potential for heterogeneously-catalyzed organic synthesis. However, the architecture of mononuclear metal species stabilized on solid supports may not be optimal in complex molecule transformations due to oversaturated coordination/limited coordination space. Exploiting synergies between active sites by controlling their proximity through carrier and metal density engineering could enable enzyme-like cooperative behaviour. This article introduces a new class of geminal-atom heterogeneous catalysts (GAC), which pair low-valence single-atom sites in specific coordination and proximity. Regularly separated nitrogen-related anchoring groups with delocalized π-bond nature in a polymeric carbon nitride host permits the synthesis of Cu geminal sites with a magic ground-state separation of ~0.4 nm at high metal density. The dynamic coordination of individual Cu sites in GAC enables a cooperative bridge-coupling pathway with a low activation barrier of 0.18 eV, leading to unprecedented performance in numerous C-X (X = C, N, O, etc.) coupling bond formations in terms of activity, selectivity and stability. In-situ characterization and quantum-theoretical studies confirm the efficient activation of the reactants over geminal metal sites. This step is not possible over SAC featuring mononuclear analogues, rendering them inactive. The use of earth-abundant and low-carbon-footprint heterogeneous catalysts for the one-pot synthesis of pharmaceutical compounds and translation to continuous flow demonstrates the broad scope of GAC for the sustainable manufacture of valuable chemicals.

Main

Transition-metal-catalyzed organic syntheses, typically exploiting homogeneous organometallic complexes, are critical in the fine-chemical and pharmaceutical industries (*1-3*). Despite their huge success, concerns arising from the use of homogeneous catalysts include their high production costs and the environmental impact associated with challenges in product separation and purification, and catalyst recycling, especially for precious metals catalysis (*4, 5*). In this context, the development of heterogeneously-catalyzed processes is highly attractive for large-scale production, facilitating catalyst separation and recovery and offering improved adaptability for continuous flow synthesis (*6, 7*). The potential advantages have triggered extensive studies of immobilized organometallic complexes and functionalized metal nanocatalysts (*8*). However, their practical applicability is not yet demonstrated due to insufficient activity, selectivity, or stability in many reactions, primarily attributed to poor control of active site structure or weak interactions with supports (*9*).

Single-atom heterogeneous catalysts (SAC), integrating well-defined mononuclear sites anchored on suitable carriers, attract growing attention for their potential to overcome the shortcomings of immobilized molecular and supported nanocrystal catalysts (*10-12*). The carrier design must ensure the stability of metal centres while permitting their adaptive coordination to fulfil the catalytic cycle and achieve enzyme-like specific activity. Nonetheless, the strong interaction between the metal centre and the carrier required to prevent metal detachment or aggregation typically leads to high coordination numbers, limiting its capacity to activate multiple substrates simultaneously (*13, 14*). These seemingly conflicting requirements have prompted debate over whether mononuclear sites provide the optimal architecture for complex molecule transformations. Some researchers have postulated that tailored multinuclear sites may be more efficient, but controlled synthesis routes for other low-nuclearity catalysts remain limited (*15*). An alternative approach would be to exploit cooperativity between metal centres in SAC by controlling their proximity.

Here, we develop a new class of *geminal-atom catalysts* (GAC) consisting of pairs of regularly separated single-atom Cu sites. The use of a nanocrystalline polymeric carbon nitride carrier permits precise control over the proximity of metal centres.

Catalytic evaluation in a broad range of cross-coupling reactions, including azide-alkyne cycloaddition, carbon-carbon, and carbon-heteroatom bond formation, demonstrates the superior performance of GAC compared to conventional SAC with a similar metal density based on a nitrogen-doped carbon host. The results show that GAC overcome a long-standing issue of sluggish oxidative addition in copper catalysis, which has limited the scope of copper compared to palladium in cross-coupling chemistry, despite its lower cost and carbon footprint. Detailed analysis of the structure and mechanism confirms the cooperativity of dynamic metal centres in the geminal sites, enabling the efficient activation of substrates through a bridge coupling mechanism. Further demonstration in the synthesis of biorelevant and pharmaceutical compounds and translation to continuous flow illustrate the broad potential of GAC to produce complex molecules in a more environmentally benign manner.

A stepwise ion exchange and ligand removal strategy was devised for the synthesis of low coordinate geminal metal atoms exploiting the abundant and periodic presence of N-H functional groups as metal coordination sites in polymeric carbon nitride (PCN, **Fig. 1A**) (*16, 17*). Here, a standard protocol was followed to synthesize PCN (as described in Methods), which is composed of polymeric heptazine chains that assemble to create layers. Upon introduction, Cu single atoms replace H atoms, as confirmed by the almost completely reduced intensity of N-H group related vibration bands of PCN (**Fig. 1B**) and are further stabilized by neighbouring N atoms (*18*). Annular dark field scanning transmission electron microscopy (ADF-STEM, **Fig. 1C**) acquired over ultra-high density Cu_g/PCN (18.3 wt.% Cu) reveals a high concentration of metal atoms, which tend to form regularly-spaced pairs (termed as geminal Cu) with an average Cu-Cu distance of ~0.4 nm. The incorporation of Cu atoms appears to link adjacent PCN polymeric chains into a 2D organic-metal lattice, which transforms the twisted stacking motifs into ordered planar structures (**Fig. S1**). As a result, PCN decorated with a high density of Cu single atoms can be exfoliated into atomically thin nanoflakes, ensuring the full accessibility of active sites for catalyzed reactions. Elemental mapping using energy-dispersive X-ray spectroscopy (EDS) and powder X-ray diffraction (XRD) measurements also confirm the uniform metal dispersion and the absence of nanoparticles or clusters in Cu_g/PCN (**Fig. S1**). Consistently, the Fourier transformed extended X-ray absorption fine structure (EXAFS, **Fig. 1D** and **Table S1**) spectrum reveals a dominant feature centred at 1.5 Å and a weak peak at around 2.2 Å,

corresponding to the first shell Cu-N and the second shell Cu-C bond lengths, respectively. A prominent pre-edge feature in the experimental Cu K-edge can be assigned to 1s $\rightarrow 4p_{xy}$ transition, indicative of a diagonal coordinated Cu (*19*). To confirm the atomic structure of the Cu sites, DFT calculations were conducted to identify possible models and simulate their corresponding XANES spectra. Among all the proposed structures (**Fig. S2**) (*20*), the one consisting of heptazine chains shows the best agreement with experimental Cu K-edge XANES spectrum (**Fig. 1E**). Such a diagonally coordinated N-Cu-N structure endows a Cu valence state of +1, which is further confirmed by X-ray photoelectron spectroscopy (**Fig. S1**) and electron paramagnetic resonance spectroscopy (EPR, **Fig. S1**).

To assess the substrate scope of the Cu_g/PCN catalyst, various (hetero)aryl iodides and bromides with different electronic and/or steric attributes were examined under standard conditions (**Fig. S3** and **Fig. S4**). The catalytic performance of Cu_g/PCN was initially evaluated for C-C, C-N, C-O, and C-S bond formation under ligand free conditions, where only the base, solvent, and catalyst are needed. The results prove Cu_g/PCN to be an efficient heterogeneous catalyst transforming the reactants to targeted products on various cross-coupling systems with a high selectivity and yield (**Fig. 2**), outperforming Cu nanocatalysts and even benchmarked homogeneous cuprous iodide at the same molar equivalent of copper (**Table S2**). Aryl iodides and bromides bearing either electron-rich or electron-deficient aryl units are effective substrates, affording cross coupling products in 60 to 90% yield (**1** to **56**). The functional (i.e., hydroxyl and amino) substituents on phenyl ring are tolerated well, which usually would not work in transition-metal-catalyzed transformations, a useful feature concerning further synthetic manipulation (**10, 11, 30**). In addition, the fluorinated alcohols (**19**, **20**) and the deuterated methanol (**23**, **24**) also work well in the C-O coupling reaction. Notably, Cu_g/PCN delivers a high yield and even better regioselectivity than the homogeneous cuprous iodide catalysis in *N*-arylation of imidazoles (**37**, **48**, **49**, **Fig. S5**). Furthermore, Cu_g/PCN also demonstrated efficient performance for azide-alkyne cycloaddition, a reaction known to involve two metal centres, with yields from 88 to 94% (**Fig. S6**) (*22*).

To confirm the unique site cooperativity in the GAC, a series of Cu single-atom catalysts (Cu_1/PCN) with different Cu contents ranging from 0.2-18.3 wt.%, where the ratio of monomeric to geminal Cu(I) sites is expected to decrease upon increasing the Cu content in the sample. The atomic Cu dispersions with varying metal content in the

Cu_1/PCN catalysts are directly imaged by ADF-STEM (**Fig. S7**), revealing increasingly populated atomic features and increasing numbers of geminal sites. The gradual decrease of N-H vibrational bands observed by FTIR spectroscopy confirms the progressive exchange of N-H groups in PCN with increasing Cu content (**Fig. S7**). Meanwhile, Cu K-edge XANES and EXAFS and XPS spectra evidence the identical chemical state of each Cu regardless of the metal content (**Fig. S8**). Analysis of the charge density distributions and partial density of states (PDOS) of monomeric and geminal Cu sites reveal the identical electronic structure, as well as the absence of a direct interaction between metal centres in neighbouring sites (**Fig. S9**). The catalytic performance of Cu_1/PCN catalysts with different Cu contents for the C-N, C-O bond formation and azide-alkyne cycloaddition were evaluated using the same amount of Cu (2 mol%, **Table S3**), respectively. Similar trends are observed in all cases, the product yields correlate with the metal content increasing from zero in the sample containing 0.2 wt.% Cu, where all the Cu(I) sites are isolated monomers to around 90% over the catalyst with the highest content of geminal sites. This control experiment reveals the inability of a monomer Cu(I) to trigger the coupling reaction because of the high energy barrier for oxidative low-valent copper to Cu(III) intermediate, highlighting the necessity of a geminal Cu(I) structure. In addition, the low valence of the metal centre endowed by the diagonally coordinated N-Cu-N configuration also plays an important role in the activation of reactants. This is in stark contrast to zero activity observed over ultra-high-density single atom Cu(II) on nitrogen-doped carbon for the C-O coupling reaction, even if the catalyst contains an abundance of adjacent CuN_4 sites (**Fig. S10**) (*23*).

Given the well-documented difficulty in oxidative addition on Cu, we performed quantum-theoretical investigations (periodic and molecular models, **Fig. S11**) to explore the coupling of 4-iodobenzene with methanol to gain molecular-level understanding of the cross-bond formation mediated by Cu_g/PCN. An initiation process induced by the separate adsorption of (hetero)aryl halides (4-iodobenzene) and the partner nucleophilic reactant (methanol) over each Cu(I) atom of the geminal site. Comprehensive theoretical calculations on the plausible mechanisms reveal that the indirect C-O coupling pathway with unbonded Cu(II)···Cu(II) active sites is unfavourable, where $*OCH_3$ couples with a β-position carbon atom of the nearby aryl and subsequent migrates to the α-position (**Fig. S12**). Instead, a direct C-O coupling

pathway is preferred over directly bonded Cu(II)-Cu(II) active sites. In the direct pathway, a dynamically formed Cu_2 dimer facilitates C-O bond formation through oxidation addition and subsequent elimination of $C_6H_5OCH_3$. The unique heptazine chain structure allows for the migration of the geminal Cu (Cu_A and Cu_B) toward each other upon the adsorption of reactants (**Fig. 4A** and **Table S4**), bringing the two reactants ($*C_6H_5$ and $*OCH_3$) close enough for the direct cross-bond formation. The system naturally returns to the original state with unbonded Cu(I)···Cu(I) sites after desorption of the product (**Fig. 4C** and Supplementary **Video 1**). Such a dynamic reconfiguration of geminal Cu sites during reaction is expected to be energetically costly, which can be largely offset by electronic energy gain through orbital hybridization. Effective atomic orbital radius of Cu 4s (~ 2.2 Å) is much larger than Cu 3d (~ 1.3 Å) in the radial probability distribution (**Fig. S13**), so that the Cu_2 dimer formation is energetically compensated via Cu-Cu 4s-4s bonding.(*24*) Indeed, the 4s-4s orbital interaction between the geminal Cu(II) will cause the system to undergo a potential-energy-surface crossing from $Cu^{II}(d^9s^0)\cdots Cu^{II}(d^9s^0)$ triplet to $Cu^{II}(d^8s^1)$-$Cu^{II}(d^8s^1)$ singlet states when the 4s-4s σ-bond is formed (**Fig. 4B**).

Apart from this, our theoretical calculations also reveal that C-O coupling via direct dehalogenation and dehydrogenation of 4-iodobenzene and methanol over Cu_A and Cu_B sites in the absence of a base is energetically unfavorable, due to a large endothermicity (2.52 eV, **Fig. S14**), consistent with experimental observation. However, upon introducing the strong base potassium tert-butoxide (KO^tBu), the deprotonation of methanol (IS1→IS2, -2.41 eV) to form $*HO^tBu$ can proceed readily because of large pKa (~17) of HO^tBu, and the subsequent dehalogenation of 4-iodobenzene (IS2→IS3, 0.33 eV) is further assisted by forming KI deposit (**Fig. S15**). As-adsorbed $*C_6H_5$ and $*CH_3O$ intermediates will be formed through a spontaneous exothermic desorption of KI and HO^tBu (IS3→IS4, -1.0 eV). It is worth noting that this base aided co-adsorption process can only occur under the combination of 4-iodobenzene with methanol, neither two 4-iodobenzene nor two methanol can occur, which can explain why only cross-coupling products were obtained instead of the homo-coupling products. The calculated binding energies of $*C_6H_5$ and $*CH_3O$ on Cu atoms were -0.90 and -1.04 eV, respectively. Our calculations also show that the absorption state of individual Cu sites in GAC has negligible mutual influence, distinct from the conventional dual-atom or bimetallic complex catalysts with a strong direct or indirect metal-metal interaction.(*25,*

26) For example, when $*CH_3O$ is preadsorbed on Cu_A site, the adsorption energy of $*C_6H_5$ at the Cu_B site is around -0.94 eV. Similarly, when $*C_6H_5$ is preadsorbed on Cu_A, the adsorption energy of $*CH_3O$ on the Cu_B is calculated to be -1.08 eV. The adsorption of 4-iodobenzene and methanol on Cu sites are directly evidenced by EPR spectroscopic measurements (**Fig. S16**), where the EPR-silent Cu(I, $d^{10}s^0$) in Cu_g/PCN is oxidized to EPR-sensitive Cu(II,d^9s^0). Further analysis of the PDOS (**Fig. S17**) and variation in the Bader charge and spin density population of Cu in Cu_g/PCN shows that the valence state of Cu after absorbing $*C_6H_5$ or $*CH_3O$ become Cu(II), consistent with the EPR result. In addition, the calculated energy profile reveals the activation of 4-iodobenzene with an activation barrier larger than 0.98 eV, represents the rate-determining step for C-O coupling, consistent with experimental kinetic investigation (**Fig. S18**).

To support the theoretical picture described above, we performed in-situ XAFS and EPR experiments to trace the chemical state and binding evolution of Cu species. The chemical state change of Cu_g/PCN during the C-O cross-coupling reaction cycle was clearly seen by Cu K-edge XANES measurements (**Fig. 4A**). A distinct weakening of the feature peak at 8983 eV and an increase of the main peak at 8996 eV indicate that the valence state of Cu increases during the reaction, which is related to the successful adsorption of 4-iodotoluene or methanol. Correspondingly, the intensity of the main peak related to the first coordination sphere in the Fourier transformed EXAFS spectra increases, evidencing the increased coordination number of Cu (**Fig. 4B**). The change in the chemical state of Cu during the reaction cycle is further elucidated by in-situ EPR spectroscopy (**Fig. 4C**). EPR-silent Cu (I) is first oxidized to EPR-sensitive Cu (II) with a gradually enhanced signal intensity and then reduced to the original Cu (I) state during a complete reaction process, in line with the in-situ XAFS results.

The compatibility of the GAC bridge coupling protocol was further applied to bio-relevant molecules. As demonstrated in **Fig. 5A**, the representative examples of L-menthol, stigmasterol, DL-isoborneol, 1,2,3,4-diacetone galactose and as the substrate partners, as well as the large-scale synthesis of drug-like p-arylthio aniline smoothly delivered the corresponding products (**57** to **63**) in good to excellent yields, highlighting the applicability of the Cu_g/PCN catalyst for the late-stage modification of complex molecules. To demonstrate the utility of this new heterogeneous catalysis system with respect to drug discovery, we focused on the batch synthesis of pharmaceutically active

compounds in multi steps or one pot manner (**Fig. 5B**). The reactions starting from commercially available substrates and under the designed synthesis process, the pharmaceuticals can be obtained in 64 to 80% overall yields (**64** to **67**).

The major advantage of using heterogenous catalysts lies in their recoverability and reusability. Cu_g/PCN demonstrated an excellent durability and recyclability in C-O coupling reaction, as shown in **Fig. S19**. The drop in yield over the first few cycles stems from the deposition of insoluble salts (KI) on the surface of catalyst that may block the active Cu sites. The high performance could be easily restored after removing the adsorbed salt by washing with deionized water. Consistently, ICP-AES analysis of the used catalyst confirms the virtually identical amount of Cu to the fresh Cu_g/PCN, accompanied by the absence of any detectable Cu ions remaining in solution. The ADF-STEM image acquired over the used Cu_g/PCN catalyst shows a high density of atoms and no visible nanoparticle aggregation was detected, suggesting that the atomic dispersion of copper species was preserved after the catalytic reaction (**Fig. S20**). FTIR, XRD, XPS, Cu K-edge XANES and EXAFS analysis also revealed the identical atomic structures of Cu in the used catalyst to the fresh Cu_g/PCN (**Fig. S20**). In addition, the coupling of 4-iodotoluene with ethanol occurred in the presence of 0.01 mol% Cu (Cu_g/PCN) producing the coupled product in 80% yield, corresponding to a turnover number (TON) of 8000, a value almost two orders of magnitude higher than the common homogeneous copper-catalyzed cross-coupling of an aryl halide with aliphatic alcohol.(*21*) It worth noting that the obtained TON value is likely underestimated due to the active site blockage by the deposition of insoluble salts as revealed in the recycling experiment. Furthermore, motivated by major developments to improve synthetic efficiency and the intensification of chemical processes, we translated the batch synthesis over Cu_g/PCN to a continuous flow protocol, which has several advantages in terms of automation and process optimization (**Fig. S21**) (*27*). Evaluation in a custom-made packed-bed reactor evidenced a stable gradient production of ethoxybenzene under varying flow speeds (**Fig. 5C**) and a constant production of 1-(4-methylbenzyl)-4-phenyl-1H-1,2,3-triazole on stream for more than 144 h with no obvious variation in selectivity or yield (**Fig. 5D**), as well as the negligible leaching of Cu ions into the solution compared to commercially available copper tube flow reactors (inset of **Fig. 5D**).

In summary, we presented the design of geminal metal single atoms catalysts anchored on polymeric carbon nitride, demonstrating their broad potential for heterogeneously-catalyzed cross-coupling reactions. The regular structure of polymeric carbon nitride enabled the formation of copper geminal sites, which were maximized at high metal densities, via a simple ion exchange and activation process. As confirmed by multiple analyses, the specific proximity of two paired low valent and electronically-isolated geminal metal centres permitted a cooperative bridge cross-coupling mechanism leading to greatly enhanced efficiency compared to the conventional monomeric sites in single-atom catalysts. This enabled the one-pot synthesis of several complex molecules including biorelevant and pharmaceutical compounds in high yields. The catalysts exhibited high stability and could be readily translated to flow processes. The well-defined geminal metal structure permitted deduction of the involvement of intermediate states by complementary experimental and theoretical analysis that have previously eluded mechanistic studies. The geminal atom catalysts offers a useful approach to solve the long-standing oxidative addition challenge of copper-based heterogeneous catalysts, enabling the wide design of environmentally benign organic synthesis by adjusting the type and combination of the geminal metals.

Acknowledgments

J. Lu acknowledges the support from MOE Tier 2 (MOE2019-T2-2-044 and MOE-T2EP50121-0008) and MOE (Singapore) through the Research Centre of Excellence program (grant EDUN C-33-18-279-V12, I-FIM). S.M. and J.P.-R. acknowledge funding from the NCCR Catalysis, a National Centre of Competence in Research funded by the Swiss National Science Foundation. Jun.L acknowledges the financial support by the National Natural Science Foundation of China (Grant 22033005) and the Guangdong Provincial Key Laboratory of Catalysis (No. 2020B121201002). Computational resources were supported by the Center for Computational Science and Engineering (SUSTech) and Tsinghua National Laboratory for Information Science and Technology.

Author contributions

X.H. and J.Lu. conceived the idea and designed the study. X.H. performed materials synthesis. Yang.Z. and X.H. performed the activity test. S.X. performed the XAFS measurement and structure analysis. X.Z. and Y.C. performed the electron microscopy

experiments and data analysis. X.L. and M.W. performed the continuous flow synthesis. Q.Y. and N.G. carried out theoretical calculations under the supervision of Jun.L. and C.Z. All authors contributed to writing the manuscript.

Competing interests

The authors declare no competing interest.

References

1. C. Bolm, M. Beller, *Transition metals for organic synthesis*. (Wiley-VCH: Weinheim, 2004), vol. 1.
2. L. Brandsma, S. F. Vasilevsky, H. D. Verkruijsse, *Application of transition metal catalysts in organic synthesis*. (Springer Science & Business Media, 2012).
3. A. De Meijere, S. Bräse, M. Oestreich, *Metal-catalyzed cross-coupling reactions and more*. (Wiley-VCH Weinheim, 2014), vol. 1.
4. R. A. Sheldon, H. Van Bekkum, *Fine chemicals through heterogeneous catalysis*. (John Wiley & Sons, 2008).
5. A. Biffis, P. Centomo, A. Del Zotto, M. Zecca, Pd metal catalysts for cross-couplings and related reactions in the 21st century: a critical review. *Chem. Rev.* **118**, 2249-2295 (2018).
6. S. Vásquez-Céspedes, R. C. Betori, M. A. Cismesia, J. K. Kirsch, Q. Yang, Heterogeneous catalysis for cross-coupling reactions: an underutilized powerful and sustainable tool in the fine chemical industry? *Organic Process Research & Development* **25**, 740-753 (2021).
7. T. Tsubogo, H. Oyamada, S. Kobayashi, Multistep continuous-flow synthesis of (R)-and (S)-rolipram using heterogeneous catalysts. *Nature* **520**, 329-332 (2015).
8. M. Benaglia, A. Puglisi, *Catalyst immobilization: methods and applications*. (John Wiley & Sons, 2019).
9. K. F. Kalz *et al.*, Future challenges in heterogeneous catalysis: understanding catalysts under dynamic reaction conditions. *ChemCatChem* **9**, 17-29 (2017).
10. A. Wang, J. Li, T. Zhang, Heterogeneous single-atom catalysis. *Nat. Rev. Chem.* **2**, 65-81 (2018).
11. X. Cui, W. Li, P. Ryabchuk, K. Junge, M. Beller, Bridging homogeneous and heterogeneous catalysis by heterogeneous single-metal-site catalysts. *Nat. Catal.* **1**, 385-397 (2018).
12. W.-H. Li, J. Yang, D. Wang, Y. Li, Striding the threshold of an atom era of organic synthesis by single-atom catalysis. *Chem*. **8**, 119-140 (2022).
13. S. K. Kaiser, Z. Chen, D. Faust Akl, S. Mitchell, J. Pérez-Ramírez, Single-Atom Catalysts across the Periodic Table. *Chem. Rev.* **120**, 11703-11809 (2020).
14. Z. Li *et al.*, Well-defined materials for heterogeneous catalysis: from nanoparticles to isolated single-atom sites. *Chem. Rev.* **120**, 623-682 (2019).
15. H. Yan, C. Su, J. He, W. Chen, Single-atom catalysts and their applications in organic chemistry. *J. Mater. Chem. A* **6**, 8793-8814 (2018).

16. T. Tyborski *et al.*, Crystal structure of polymeric carbon nitride and the determination of its process-temperature-induced modifications. *Journal of Physics: Condensed Matter* **25**, 395402 (2013).
17. F. Fina, S. K. Callear, G. M. Carins, J. T. Irvine, Structural investigation of graphitic carbon nitride via XRD and neutron diffraction. *Chemistry of Materials* **27**, 2612-2618 (2015).
18. B. H. Stuart, *Infrared spectroscopy: fundamentals and applications*. (John Wiley & Sons, 2004).
19. M. Sendzik, M. J. Pushie, E. Stefaniak, K. L. Haas, Structure and affinity of Cu (I) bound to human serum albumin. *Inorganic chemistry* **56**, 15057-15065 (2017).
20. F. K. Kessler *et al.*, Functional carbon nitride materials-design strategies for electrochemical devices. *Nature Reviews Materials* **2**, 1-17 (2017).
21. S. Bhunia, G. G. Pawar, S. V. Kumar, Y. Jiang, D. Ma, Selected copper-based reactions for C-N, C-O, C-S, and C-C bond formation. *Angew. Chem. Int. Ed.* **56**, 16136-16179 (2017).
22. B. Worrell, J. Malik, V. V. Fokin, Direct evidence of a dinuclear copper intermediate in Cu (I)-catalyzed azide-alkyne cycloadditions. *Science* **340**, 457-460 (2013).
23. X. Hai *et al.*, Scalable two-step annealing method for preparing ultra-high-density single-atom catalyst libraries. *Nat. Nanotechnol.* **17**, 174-181 (2022).
24. J.-M. Zuo, M. Kim, M. O'keeffe, J. Spence, Direct observation of d-orbital holes and Cu-Cu bonding in Cu_2O. *Nature* **401**, 49-52 (1999).
25. W. Zhang *et al.*, Emerging Dual-atomic-site catalysts for efficient energy catalysis. *Adv. Mater.* **33**, 2102576 (2021).
26. J. Campos, Bimetallic cooperation across the periodic table. *Nat. Rev. Chem.* **4**, 696-702 (2020).
27. B. Gutmann, D. Cantillo, C. O. Kappe, Continuous-flow technology-a tool for the safe manufacturing of active pharmaceutical ingredients. *Angew. Chem. Int. Ed.* **54**, 6688-6728 (2015).

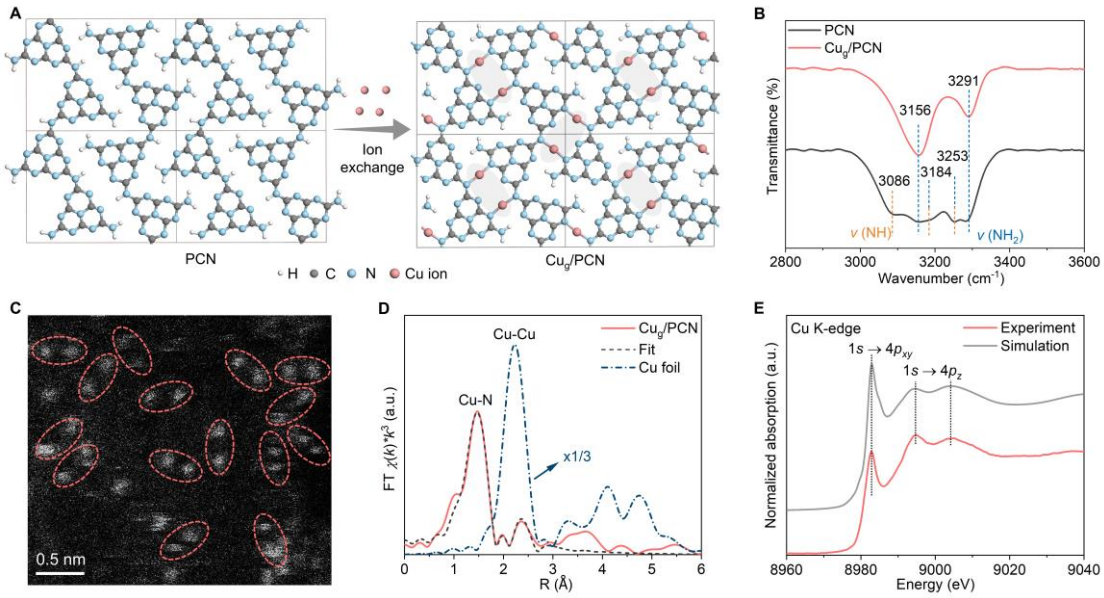

Fig. 1. Synthesis and characterization of Cu$_g$/PCN. (**A**) Strategy for the preparation of Cu$_g$/PCN geminal atom catalysts based on the periodic crystal structure of the host. (**B**) FTIR spectra of PCN and Cu$_g$/PCN. (**C**) Atomic-resolution ADF-STEM image (scale bar: 1 nm, geminal Cu structures are circled). (**D**) Cu K-edge Fourier transformed EXAFS spectra, and (**E**) the experimental high-resolution XANES spectra compared with the calculated XANES data of optimized DFT-modelled structure of Cu$_g$/PCN.

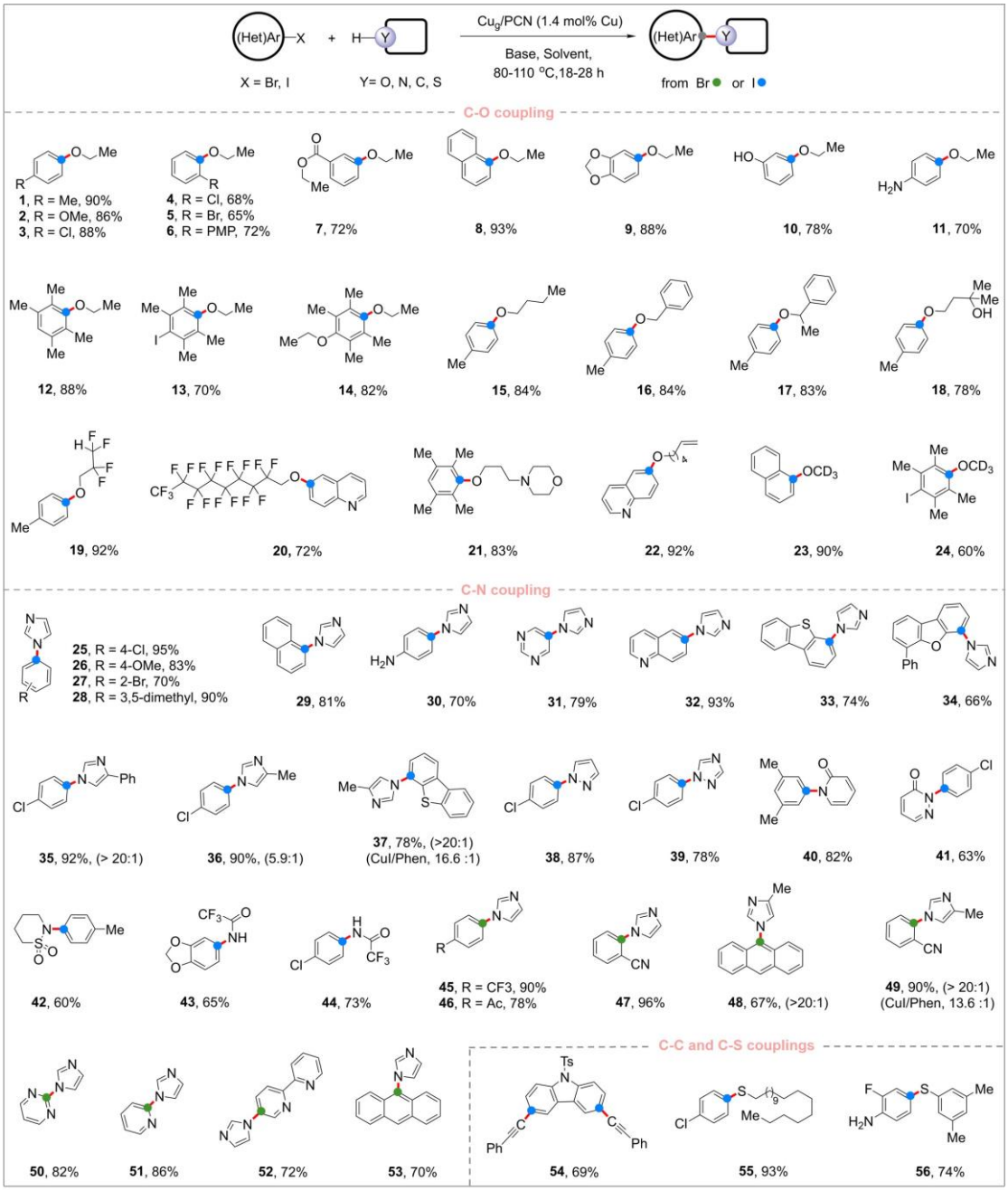

Fig. 2. Substrate scope of Cu$_g$/PCN catalyzed cross-couplings. Product yields obtained in Cu$_g$/PCN catalyzed C-O, C-N, C-C, and C-S bond formations with large scope of (hetero) aryl halides.

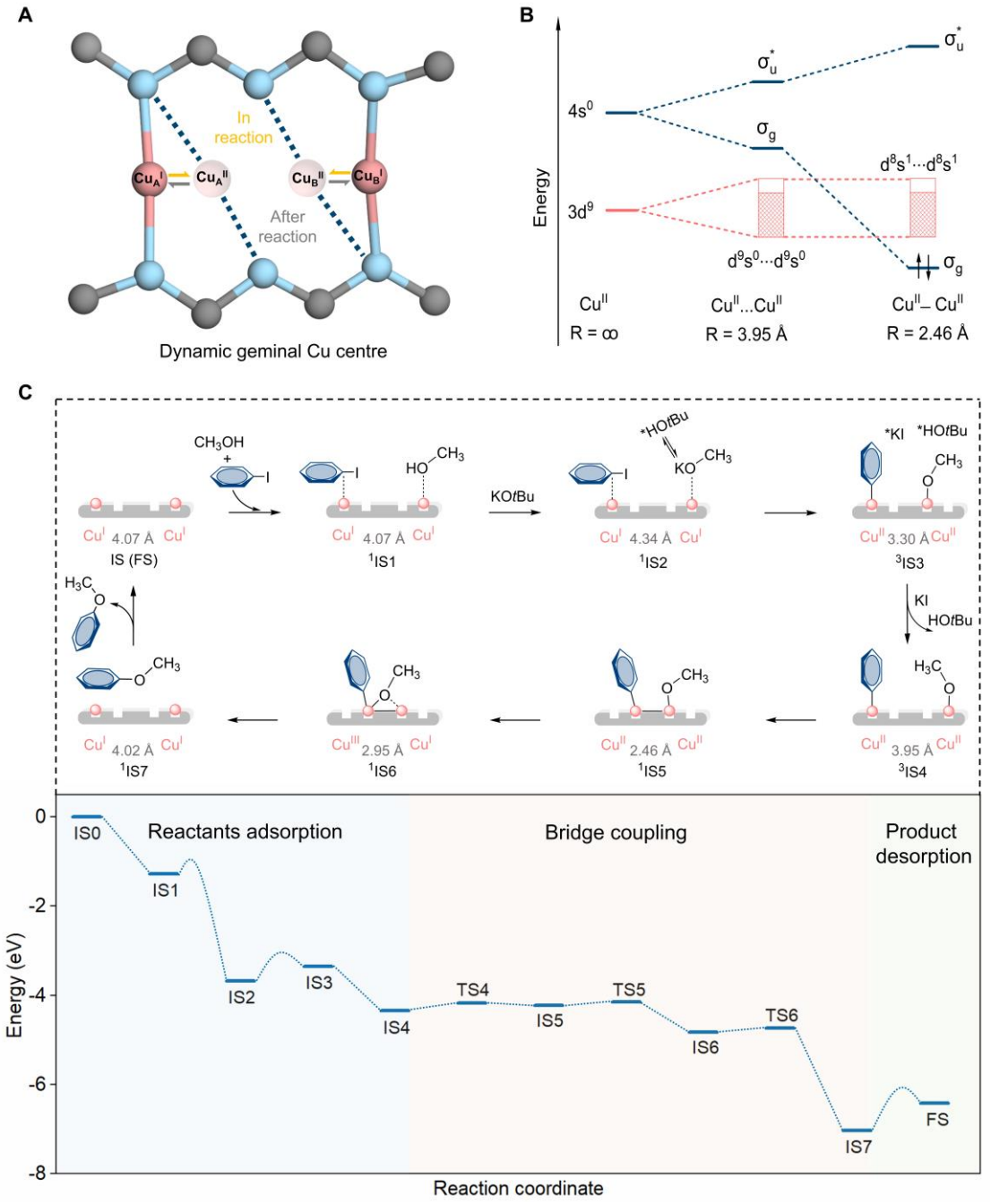

Fig. 3. Mechanistic investigation of C-O coupling over Cu_g/PCN. (**A**) Schematic of the dynamic coordination of geminal Cu active centres. (**B**) The energy level of Cu (II)…Cu (II) interaction with increasing proximity from ∞ to 2.46 Å. (**C**) The proposed reaction mechanism and the calculated energy profiles for C-O bond formation mediated by Cu_g/PCN. The spin state, valence state, and Cu···Cu distance are marked in the figure.

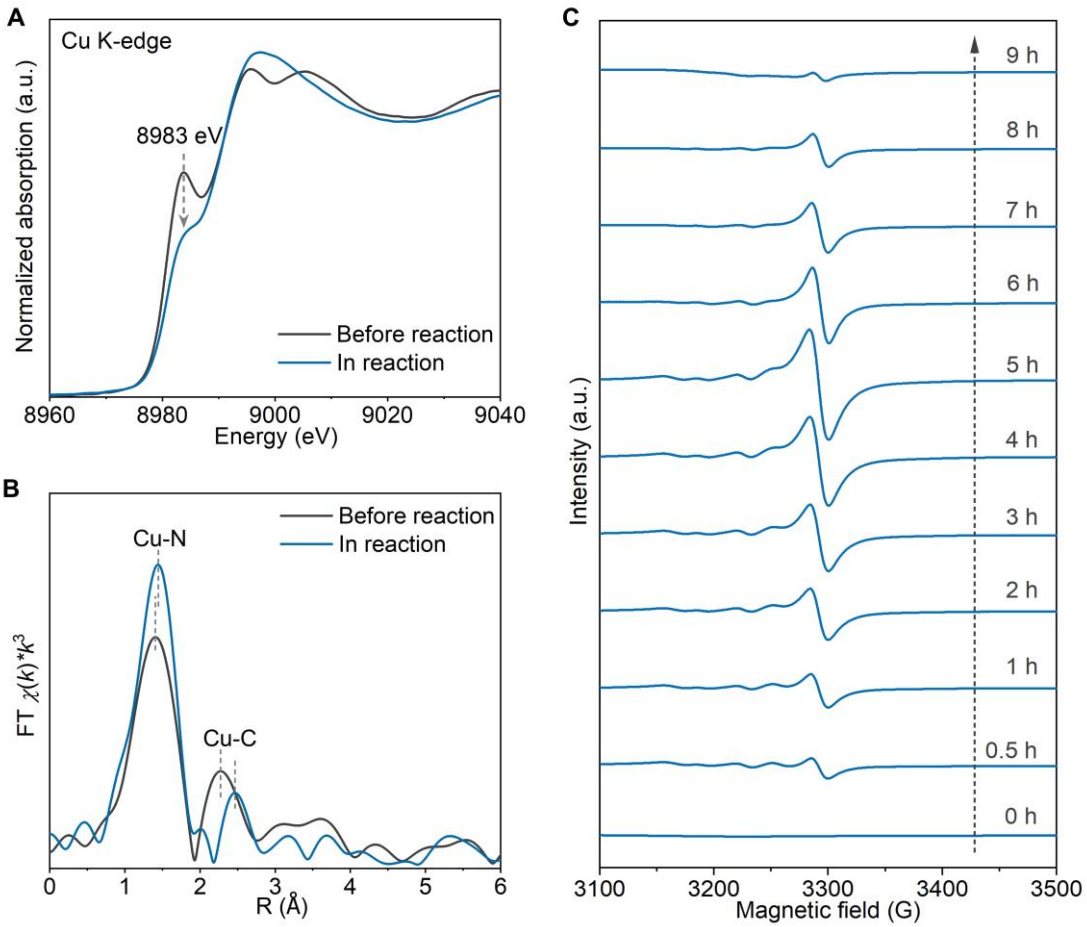

Fig. 4. In-situ XANES and EPR spectra during C-O coupling reaction. In-situ Cu K-edge XANES (**A**) and Fourier-transformed EXAFS (**B**) spectra of Cu_g/PCN catalyst measured before and in the C-O coupling reaction, respectively. (**C**) In-situ EPR spectra of Cu_g/PCN recorded at different times in the C-O coupling reaction.

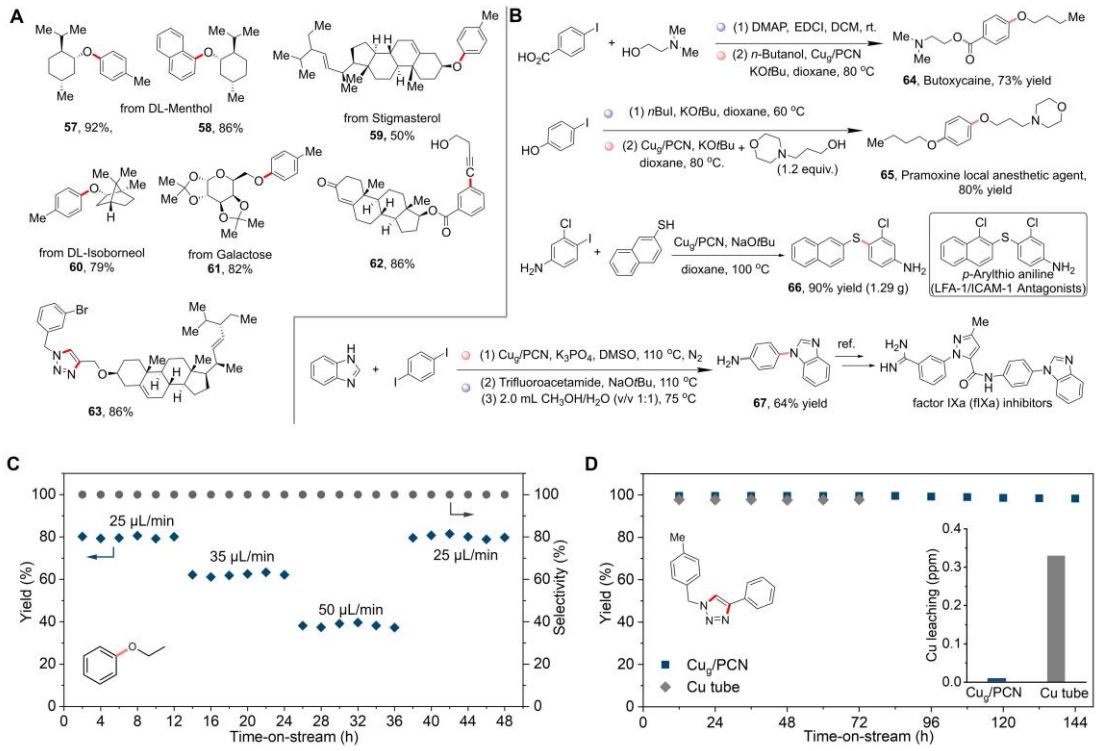

Fig. 5. Cu$_g$/PCN catalyzed biorelevant molecule and continuous flow synthesis. (**A**) Synthesis of bio-relevant molecules (57-63) from natural products. (**B**) Synthesis of pharmaceutical compounds (64-67) in multi steps and one-pot manner. (**C**) Continuous flow synthesis of ethoxybenzene over Cu$_g$/PCN under various flow speed. (**D**) The yield of 1-(4-Methylbenzyl)-4-phenyl-1H-1,2,3-triazole as a function of time-on-stream over Cu$_g$/PCN and Cu tube, respectively. The inset shows the measured concentration of Cu ions leached into the solution at the end of each reaction.